Performance Enhancement for m-Sequence and Hadamard Code SAC-OCDMA Systems Based on Narrowband Filters

Sokaina Boukricha, Afaf Bouzidi, Kamal Ghoumid, El Miloud Ar-Reyouchi, Réda Yahiaoui, Omar Elmazria

Noname manuscript No.
(will be inserted by the editor)

Performance enhancement for m-sequence and Hadamard code SAC-OCDMA systems based on narrowband filters

Sokaina Boukricha · Afaf Bouzidi · Kamal Ghoumid · El miloud Ar-Reyouchi · Réda Yahiaoui · Omar Elmazria

Received: date / Accepted: date

Abstract In this paper, we examine the performance of a Spectral Amplitude Coding-Optical Code Division Multiple Access (SAC-OCDMA) system using two different codes: m-sequence and Hadamard. Fiber Bragg Grating (FBG) filters and balanced detection technique are employed for performance enhancement. The system performance is evaluated in terms of Quality factor (Q), Bit Error Rate (BER) and Signal-to-Noise Ratio (SNR) as a function of number of users and fiber distance. The achieved results using a co-simulation Matlab-Optisystem version 17 are considered as improvements over previous works found in the literature. The results corresponding to a first comparative study of the system performance using the both code sequences show that using Hadamard code yields a better BER performance than using m-sequence code. This led us to study the performance of the proposed system for a larger number of users using the Hadamard code of length L=32 (m=5). The simulation results reveal that at a data rate of 100 Mbits/s and a FBG bandwidth of 0.4 nm, the suggested SAC-OCDMA system may support up to 13 users with a transmission distance of 5 Km. The obtained results also show that a distance of 45 Km can be used for a number of users up to 8 with BER=9.8E-09, Q=5.82 and SNR=20.71 dBm.

Keywords SAC-OCDMA · m-sequence code · Hadamard code · Narrowband filters · Q-factor · BER · SNR

Sokaina Boukricha
Department of Electronics, Informatics and Telecommunications, ENSAO, Mohammed Premier University. Oujda. Morocco E-mail: s.boukricha@ump.ac.ma

Afaf Bouzidi
Department of Electronics, Informatics and Telecommunications, ENSAO, Mohammed Premier University. Oujda. Morocco

Kamal Ghoumid
Department of Electronics, Informatics and Telecommunications, ENSAO, Mohammed Premier University. Oujda. Morocco E-mail: k.ghoumid@ump.ac.ma

El miloud Ar-Reyouchi
Department of Telecommunication and Computer Science, Abdelmalek Essaadi University, Tétouan, Morocco

Réda Yahiaoui
NanoMedicine Lab, Therapeutic Imagery, Franche-Comte University, Besançon, France

Omar Elmazria
Université de Lorraine, CNRS, IJL, F-54000, Nancy, France

1 Introduction

Recently, optical telecommunication systems have seen the emergence of new technologies, namely: Multiple Access technologies allowing the sharing of data between several users with high bandwidths, improved transmission capacity and high service security [1].
OCDMA is one of the Multiple Access technologies that has been given special importance compared to other existing techniques such as: WDM, TDM, FDM... thanks to their ability to transmit data without requiring any access synchronization necessitating complicated and costly electronic protocols [2,3]. They take the advantage of an all-optical process, a high level of service security and the availability of simultaneous users [4,5]. Indeed, CDMA is a spread-spectrum technique based on the principle of distributing the power of the transmitted signal over the entire bandwidth, which is much wider than that required to transmit the desired signal [6].
Furthermore, the performance of an OCDMA system is limited by many kinds of noise, such as shot noise,

thermal noise and MAI resulting from overlapping signals of different existing users [7,8]. The SAC-OCDMA is one of the OCDMA codes that has been implemented and deserves special attention because of its significant ability to reduce Multiple Access Interferences (MAI) [9–11].

The SAC-OCDMA technique is essentially based on encoding and decoding the optical signal utilizing a variety of detection techniques and different fixed-phase cross-correlation code sequences [12,13].

On the one hand, many researches have been focused on the use of encoding techniques such as SAC-OCDMA encoding based on arrayed waveguide-gratings (AWGs) and SAC-OCDMA encoding using optical demultiplexers and multiplexers (WDM)[14,15]. Similarly, detection techniques such as AND subtraction detection, modified AND subtraction detection, and balanced detection approach have been implemented [16,17]. These techniques contribute significantly to the performance improvement of SAC-OCDMA systems because they are based on schemes that minimize the effect of multiple access interference. Each technique is characterized by a specific operating principle. The balanced detection technique is based on splitting the received signal into two branches: the upper branch has the same spectral response as the encoder, and the lower branch has the complementary spectral response. Then a subtractor is used to calculate the difference in correlation between the resulting signals of the two branches. The AND subtraction detection is based on dividing the received signal into two parts, one part that has a filter structure identical to that of the encoder and the other part that has AND filter structures. The two signals are subjected to an AND operation to detect overlapping wavelengths and then sent to a subtractor to remove the overlapping wavelengths from the desired code. Finally, the modified-AND subtraction detection is based on dividing the received signal into two parts; one part corresponds to the decoder and the other part corresponds to the AND decoder. The decoder consists of filters in a parallel structure whose spectral response is adapted to the active user, and the AND decoder consists of filters with spectral response that corresponds to the overlapping data of existing interferers.

Following our promising work already carried out on experimental realizations of Fiber Bragg gratings using Lithium Niobate by the E-beam lithography technique, we have been able to realize a waveguide which allows to have a good reflectivity around 100% and a very narrow band (< 1 nm) [11]. Therefore, in this work, we have chosen to rely on Fiber Bragg Gratings for both encoding and decoding the SAC-OCDMA system using balanced detection technique. The use of such a filter allows for achieving good performance in terms of MAI reduction since FBGs allow the reflection of very specific wavelengths [18–20].

On the other hand, several signature codes have been implemented for the encoding and decoding process in SAC-OCDMA systems. These include the m-sequence code, Hadamard code, MQC (Modified Quadratic Congruence) Code, EDW (Enhanced Double Weight) code, MFH (Modified Frequency-Hopping) code, etc [21–25]. However, these codes are limited in terms of certain parameters such as the code length, the possible code sequences to be constructed and the maximum cross-correlation value which usually depends on the code weight. It's worth noting that the Hadamard code is often characterized by its shorter length when compared to other codes [26].

SAC-OCDMA system performance based on Hadamard code was investigated in terms of BER and transmission quality with use of Dispersion Compensation Fiber Bragg grating (DCFBG) and Erbium Doped Fiber Amplifier (EDFA). However, the results presented showed that the number of users allowing an acceptable BER is limited to 7 users [27].

The purpose of this work is first to compare the performance of the SAC-OCDMA system of ten users using m-sequence and Hadamard codes, and second to simulate a larger number of users using the code proving better performance.

The presented results are obtained using a co-simulation Matlab-Optisystem and are considered to be an improvement over other works found in the literature studying the SAC-OCDMA systems with different encoding/decoding and detection techniques [28,2,20].

The present paper is organized as follows. Section 2 includes a description of the SAC-OCDMA architecture. In section 3, a detailed performance analysis of the studied system is introduced. Next, Section 4 is devoted to the simulation setup, results and discussions. Finally, a conclusion is provided in Section 5.

2 SAC-OCMDA architecture

The block diagram of multi-users SAC-OCDMA system is illustrated in Fig.1 and consists of two main blocks: the transmitter and the receiver. Each user's transmitter includes an incoherent broadband source emitting an optical signal that will be modulated by an external modulator. Then, an encoder is implemented to filter the modulated signal and realize the SAC-OCDMA concept by attributing a unique code to each user. The encoder consists of a series of FBGs having the same bandwidth but different wavelength value as illustrated in Fig.2. It filters specific wavelengths that

are emitted by the incoherent broadband optical source. The encoded signals are collected using an optical combiner and transmitted through the optical fiber. The receiver block consists of a decoder, a complementary decoder (c-decoder), two photodiodes (PD and c-PD) and a subtractor. The received signal is divided into two branches: the upper branch consisting of a decoder with a spectral response similar to that of the encoder used on the transmitter side, and the lower branch consisting of a c-decoder with a complementary spectral response. Finally, the decoded signals are transmitted to the two photodiodes electrically connected in opposition, and then to the subtractor.

3 Performance analysis

The aim of this section is to develop the BER expression of a SAC-OCDMA system by calculating the different required expressions of the mean optical power and the diverse optical noises related to the receiver signal.
The first step is to calculate the Power Spectral Density (PSD) reaching the photodiodes in the receiver block and representing the combination of the different PSDs emitted by an incoherent source and then filtered by the various elements used for the coding and decoding process. the following calculations are performed according to the same procedure as in [29].

3.1 Optical Power Spectral Density (PSD)

The calculation of the PSD expressions is examined according to a procedure dealing with four different cases depending on the user's activity and inactivity. They are expressed as follow [29,30]:

$$S_0(\nu) = S\sum_{i=1}^{N_I} Y_i(\nu)H_D(\nu) \tag{1a}$$

$$S_{0C}(\nu) = TS\sum_{i=1}^{N_I} Y_i(\nu)H_{CD}(\nu) \tag{1b}$$

$$S_1(\nu) = S\left[H_E(\nu)H_D(\nu) + \sum_{i=1}^{N_I} Y_i(\nu)H_D(\nu)\right] \tag{1c}$$

$$S_{1C}(\nu) = TS\left[H_E(\nu)H_{CD}(\nu) + \sum_{i=1}^{N_I} Y_i(\nu)H_{CD}(\nu)\right] \tag{1d}$$

Where N_I represents the number of existing interferers that varies in the interval [0, K-1]; K is the number of users. $S_0(\nu)$ and $S_{0C}(\nu)$ represent the received PSDs at the photodiode (PD) and its complementary (C-PD), respectively when the required user is inactive. $S_1(\nu)$ and $S_{1C}(\nu)$ are the received PSDs at the PD and C-PD, respectively when the required user is active. $Y_i(\nu)$ is the transfer function of the encoder corresponding to the ith arbitrary interferer. $H_D(\nu)$ and $H_{CD}(\nu)$ represent the transfer functions of the decoder and the c-decoder of the required user, respectively. $H_E(\nu)$ represents the required user encoder transfer function, and T designates the transmission factor of the attenuator beside the c-detector.

3.2 Mean optical power

The mean optical power that reaches the photodiodes is given by:

$$\langle P\rangle = \int_0^{B_0} S(\nu)d\nu \tag{2}$$

Where $S(\nu)$ designates the Spectral Power Density (SPD) expressed in Eq (1), and B_0 represents the optical bandwidth of the incoherent broadband source.
Based on Eq (1) and replacing the summation term of N_I interferers having the same contribution by N_I times the contribution of one interferer, the Mean Optical Power expressions of the four cases are obtained:

$$\langle P_0\rangle = SN_I\int_0^{B_0} Y_I(\nu)H_D(\nu)d\nu \tag{3a}$$

$$\langle P_{0C}\rangle = TSN_I\int_0^{B_0} Y_I(\nu)H_{CD}(\nu)d\nu \tag{3b}$$

$$\langle P_1\rangle = S\int_0^{B_0} H_E(\nu)H_D(\nu)d\nu + SN_I\int_0^{B_0} Y_I(\nu)H_D(\nu)d\nu \tag{3c}$$

$$\langle P_{1C}\rangle = TS\int_0^{B_0} H_E(\nu)H_{CD}(\nu)d\nu + TSN_I\int_0^{B_0} Y_I(\nu)H_{CD}(\nu)d\nu \tag{3d}$$

The mean optical power corresponding to the required user after the balanced detection is given by:

$$\langle P_{user}\rangle = \langle P_1\rangle - \langle P_{1C}\rangle \tag{4}$$

Note that in the case of m-sequence code and Hadamard code, the attenuator is not required on the c-decoder side and therefore T is equal to 1. The active user mean optical power is:

$$\langle P_{user}\rangle = S\int_0^{B_0} Y_I(\nu)H_{CD}(\nu)d\nu \tag{5}$$

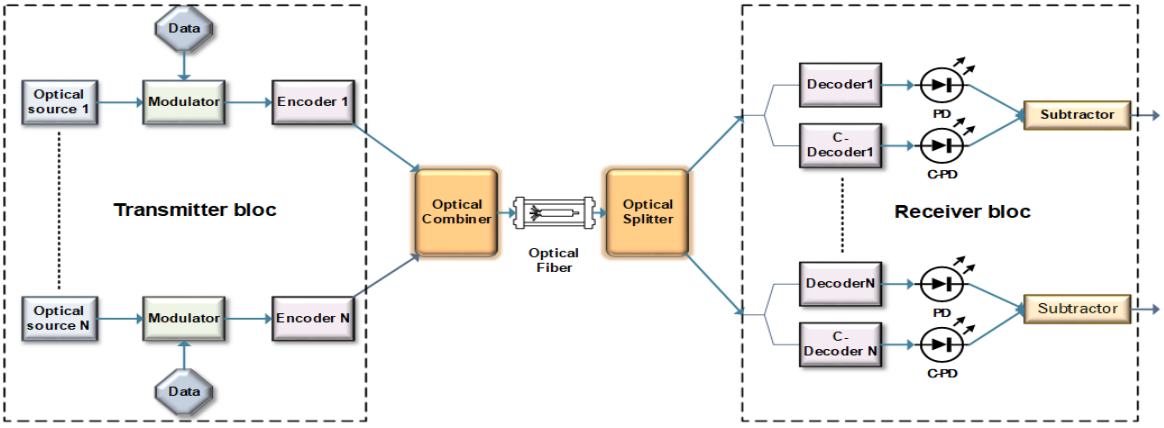

Fig. 1 SAC-OCDMA system block diagram

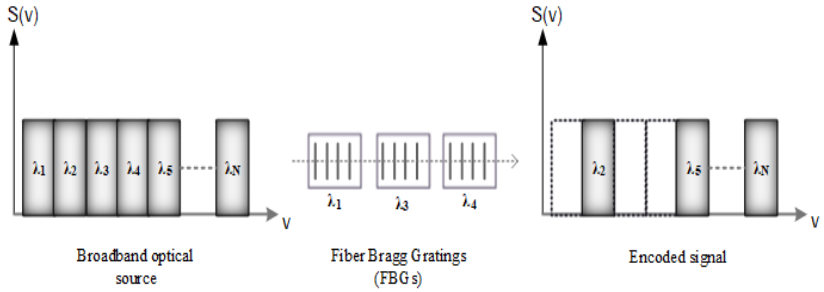

Fig. 2 Encoder based on narrowband Bragg filters

The characteristics corresponding to m-sequence code and Hadamard code are presented in Table 1.

FBG encoder and decoder

The fiber Bragg grating is amongst filters that have been widely implemented in the telecommunication field and in particular for spectral amplitude coding for OCDMA systems.It is a periodic structure that represents a periodic change of refractive index when exposed to an intense light source. Therefore, thanks to the refractive index modulation, the Bragg grating reflects a frequency band around a specific wavelength known as the Bragg wavelength, according to the following equation [31]:

$$2n_{eff}\Lambda = m\lambda_B \tag{6}$$

Where: n_{eff} is the effective index, m is the Bragg's order and Λ is the Bragg Grating period. As detailed in [31], the gain and bandwidth settings of the FBGs used in the simulations of this study are derived from the transfer function which depends on several opto-geometric parameters namely the number of periods N, the period value Λ, the duty cycle r, etc.
On the other hand, the transmission channel used in the current study is a standard single mode fiber (SMF) without the use of any amplifiers or dispersion compensators. The attenuation and dispersion factors of the optical fiber are taken into account and set to 0.25 dB/km and 18 ps/nm km, respectively, according to the ITU-T G.652 standard.
A broadband incoherent optical source is used to generate a light spectrum consisting of different wavelengths. Using the formula relating frequency and wavelength given by $f = \frac{c}{\lambda}$, the width of the frequency spectrum of the incoherent optical source is defined by [32]:

$$\Delta f = \frac{c}{\lambda^2}\Delta\lambda \tag{7}$$

Where c: the speed of light in vacuum and λ and $\Delta\lambda$ are the optical source wavelength and spectral width, respectively.
The average power spectral density (PSD) of the incoherent optical source is expressed as:

$$PSD = \frac{P_{average}}{\Delta f} \tag{8}$$

Where: $P_{average}$ is the average power of the optical source measured using a power meter component.

Table 1 Characteristics of m-sequence and Hadamard codes [29]

Code sequence	Code length (L)	Number of users(K)	Weight (w)	Cross-correlation(λ)
m-sequence	2^m-1	2^m-1	2^{m-1}	2^{m-2}
Hadamard	2^m	2^m-1	2^{m-1}	2^{m-2}

3.3 Optical noise analysis

In addition to the determination of the Mean Optical Power expression, the analysis of the optical noise is also required to calculate the BER expression.
Generally, in a SAC-OCDMA system, there are three types of optical noises, namely: Intensity noise, thermal noise and shot noise.

– The intensity noise expression ($B_0 \gg B_e$) is calculated by:

$$\sigma_{in} = \frac{2B_e}{N_{pol}} \int_0^{B_0} \left[S(\nu)\right]^2 d\nu \tag{9}$$

Where N_{pol} represents the number of polarizations of the optical source that is equal to 2 for unpolarized sources, and B_e refers to the electrical bandwidth of the balanced detector.
By substituting the terms of $S(\nu)$ given in eq (1) into eq (9), and by taking into account the intensity noise dependency on N_I, the intensity noise expression corresponding to each case is:

$$\sigma^2_{P_0|N_I} = N_I\sigma^2_{PID} + N_I(N_I-1)\left\langle\sigma^2_{PijD}\right\rangle \tag{10a}$$
$$\sigma^2_{P_{0C}|N_I} = N_I\sigma^2_{PIC} + N_I(N_I-1)\left\langle\sigma^2_{PijC}\right\rangle \tag{10b}$$
$$\sigma^2_{P_1|N_I} = \sigma^2_{PED} + 2N_I\sigma^2_{PIED} + N_I\sigma^2_{PID} + N_I(N_I-1)\left\langle\sigma^2_{PijD}\right\rangle \tag{10c}$$
$$\sigma^2_{P_{1C}|N_I} = \sigma^2_{PEC} + 2N_I\sigma^2_{PIEC} + N_I\sigma^2_{PIC} + N_I(N_I-1)\left\langle\sigma^2_{PijC}\right\rangle \tag{10d}$$

Where $\sigma^2_{PID}, \sigma^2_{PijD}, \sigma^2_{PED}$ and σ^2_{PIED} are the noise component from an interferer alone, two interferers beating together, the desired user alone and the desired user and an interferer beating together, respectively. $\sigma^2_{PIC}, \sigma^2_{PijC}, \sigma^2_{PEC}$ and σ^2_{IPEC} are the complementary noise components.

$$\sigma^2_{PID} = \frac{\sigma_0^2}{B_0}\int_0^{B_0}\left[Y_i(\nu)H_D(\nu)\right]^2 d\nu \tag{11a}$$
$$\sigma^2_{PijD} = \frac{\sigma_0^2}{B_0}\int_0^{B_0} Y_i(\nu)Y_j(\nu)\left[H_D(\nu)\right]^2 d\nu \tag{11b}$$
$$\sigma^2_{PED} = \frac{\sigma_0^2}{B_0}\int_0^{B_0}\left[H_E(\nu)H_D(\nu)\right]^2 d\nu \tag{11c}$$
$$\sigma^2_{PIED} = \frac{\sigma_0^2}{B_0}\int_0^{B_0} Y_i(\nu)H_E(\nu)\left[H_D(\nu)\right]^2 d\nu \tag{11d}$$

Where σ_0^2 represents the reference noise component that is defined by:

$$\sigma_0^2 = \frac{2B_0B_eS^2}{N_{pol}} = B_0B_eS^2 \tag{12}$$

The total intensity noise can be calculated by:

$$\sigma^2_{in} = \sigma^2_{P_0} + \sigma^2_{P_1} \tag{13}$$

– The variance of thermal noise is given by [33]

$$\sigma^2_{th} = \frac{4\kappa_\beta T_n B_e}{R_L} \tag{14}$$

Where κ_β is the Boltzmann's constant, T_n is the receiver noise temperature and R_L is the receiver load resistance.

– The variance of shot noise is defined by:

$$\sigma^2_{sh} = 2eB_e\left\langle P_{user}\right\rangle\Re \tag{15}$$

Where $\Re$ is the photodiode responsivity ($\Re = \frac{\eta e}{h\nu}$) [34]. Finally, the total optical noise of a SAC-OCDMA system is computed by summing equations (13), (14) and (15).

$$\sigma^2_T = \sigma^2_{in} + \sigma^2_{th} + \sigma^2_{sh} \tag{16}$$

3.4 SNR and BER expressions

The Signal to noise ratio is defined by:

$$SNR = \frac{\langle P_{user} \rangle^2}{\sigma_T^2} \quad (17)$$

Based on the approximation of Gaussian distribution, the Bit Error Rate (BER) is related to the SNR via the following equation [29,35]

$$BER = \frac{1}{2} erfc\left(\frac{\sqrt{SNR}}{2}\right) \quad (18)$$

Where erfc is the complementary error function.
Table 2 summarizes the corresponding expressions of the mean optical power ($\langle P_{user} \rangle$), the total optical noise (σ_T^2) and the Signal to Noise Ratio (SNR) of m-sequence code and Hadamard code.

4 Simulation setup and results

4.1 System description

The proposed SAC-OCDMA system shown in Fig.3 is composed of three blocs: transmitter bloc, transmission channel and receiver bloc.
The transmitter consists of an optical source (White Light Emitting Diode) emitting an optical power, a PRBS (Pseudo Random Bit Generator) generating the information signals using the NRZ coding and an external Mach-Zehnder modulator used to modulate the generated signal. The encoder connected to the output of the MZN modulator consists of different FBGs having different wavelengths values. It is used to encode users constituting the SAC-OCDMA system by allocating a unique code sequence to each one. The coded information signals are then transmitted over an optical fiber linked to the output of an optical combiner. The receiver bloc is made up of different decoders where the received signal corresponding to each decoder is divided into two parts: the upper part is filtered out using a decoder similar to the encoder at the transmitter and the lower part is filtered out using the complementary decoder. The decoded information signals are passed to two photodiodes converting them to an electrical signal then to a subtractor and a low pass filter in order to retrieve the signal corresponding to each user. Finally, a BER analyzer is placed at the output of the SAC-OCDMA system to analyze its performance by indicating the quality factor and the bit error rate (BER) values.

4.2 Results and discussion

The described model of SAC-OCDMA system shown in Fig.3 is simulated using Optisystem software version 17 for two different code sequences, namely: m-sequence code and Hadamard code.
First, the simulations were performed comparing the performance presented by the m-sequence code of length L=15 and the Hadamard code of length L=16, by investigating the effect of the fiber distance on the BER for different number of users. Then, based on the obtained results, we tried to rely on the code showing better performance to simulate the proposed system for a larger number of users.

4.2.1 Comparative simulation of BER performance as a function of fiber distance using the m-sequence and the Hadamard code

The variation of BER versus fiber distance at different number of users using m-sequence and Hadamard codes is respectively demonstrated in Fig.4 and Fig.5. The bit rate and the bandwidth are set at 100 Mbits/s and 0.3 nm,respectively. According to the both Figures, it is clear that as the fiber distance and the number of users increase the BER increases as well.
Figure 4 shows that at a fiber distance of 5 Km, the number of possible users with an acceptable BER of 9E-09 can be up to 9 users. Similarly, a system of 7 users performs well over a fiber distance of up to 25 Km where the corresponding BER is about 4.33E-09 . Then, for L=45 Km, the studied system is still performing well for 5 users with a BER= 1.5E-10.
Regarding the variation of BER versus fiber distance using the Hadamard code (Fig.5), and performing a similar study to that performed using the m-sequence code, it can be observed that at L=5Km and L=25 Km, the number of users offering good performance is respectively, 9 users with BER=1.51E-09 and 8 users with BER=1.44E-09. Moreover, the possible fiber distance for a SAC-OCDMA system of 7 users can be up to 35 km instead of the 25 km achieved with the m-sequence code. Finally, the studied system is indeed able to provide good BER performance for a distance up to 55 km with 5 active users. Based on the obtained results and by comparing the curves in Fig.4 and Fig.5, it can be deduced that the use of Hadamard code provides good performance and longer transmission distance compared to the m-sequence code. Thus, a larger number of users is achievable with a long transmission distance. For example, using the m-sequence code, the maximum fiber distance achieved for a system of 8 users is 10 km with a BER of 5.02E-09. However, using the

Table 2 $\langle P_{user} \rangle$, σ_T^2 and SNR expressions for m-sequence code and Hadamard code

Code sequence	$\langle P_{user} \rangle$	σ_T^2	SNR
m-sequence	$S\frac{B_0}{L}\left(\frac{L+1}{2}\right)$	$B_0 B_e S^2 \frac{L+1}{8L}(K^2+3K+2) + \frac{4k_\beta T_n B_e}{R_L} + 2eB_e S\frac{B_0}{L}\left(\frac{L+1}{2}\right)\Re$	$\frac{\frac{S^2 B_0^2}{L^2}\left(\frac{L+1}{2}\right)^2}{\frac{B_e B_0 S}{L}\left(\frac{L+1}{2}\right)\left[\frac{S(K^2+3K+2)}{4}+2e\Re\right]+\frac{4k_\beta T_n B_e}{R_L}}$
Hadamard	$\frac{SB_0}{2}$	$\frac{B_0 B_e S^2}{2}K^2 + \frac{4k_\beta T_n B_e}{R_L} + eB_e S B_0 \Re$	$\frac{\frac{S^2 B_0^2}{4}}{B_0 B_e S\left(\frac{SK^2}{2}+e\Re\right)+\frac{4k_\beta T_n B_e}{R_L}}$

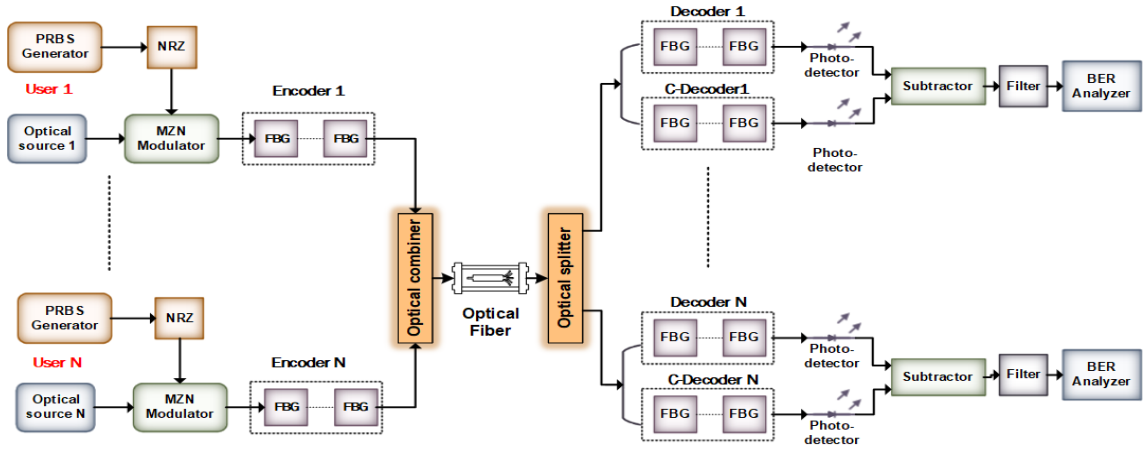

Fig. 3 SAC-OCDMA system model using FBGs filters and balanced detection technique

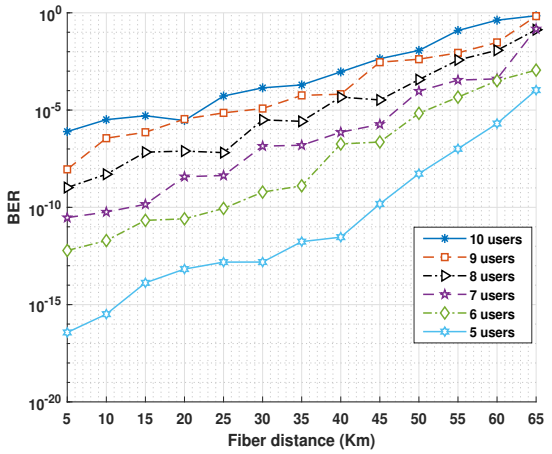

Fig. 4 BER variation versus fiber distance for different number of users for a SAC-OCDMA system using m-sequence code (L=15)

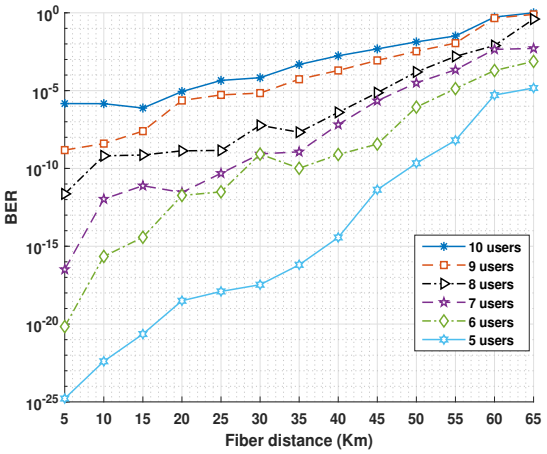

Fig. 5 BER variation versus fiber distance for different number of users for a SAC-OCDMA system using Hadamard code (L=16)

Hadamard code, a good transmission performance can be achieved over a longer distance, up to 25 Km, with a BER of 1.44E-09.

4.2.2 Performance simulation of the SAC-OCDMA system using the Hadamard code (L=32)

In this section, we are particularly interested in studying the SAC-OCDMA system using the Hadamard code of length L=32 (m=5).

The Hadamard code is one of the main codes offering good orthogonality conditions between different code sequences. It is constructed using the Hadamard matrix, an $n \times n$ square matrix whose columns and rows are orthogonal to each other [23]. The code sequences are represented by the matrix rows composed of 1 and -1 or 1 and 0.
The Hadamard matrix of order n is given by [23]:

$$H_{2n} = \begin{bmatrix} H_n & H_n \\ H_n & -H_n \end{bmatrix}$$

With $H_1 = [1]$ and $H_2 = \begin{bmatrix} 1 & 1 \\ 1 & -1 \end{bmatrix}$
Therefore, by replacing the -1's by 0's, the matrix corresponding to the Hadamard code (L=32) is defined by:

$$H_{32} = \begin{bmatrix} H_{16} & H_{16} \\ H_{16} & -H_{16} \end{bmatrix} \quad (19)$$

With:

$$H_{16} = \begin{bmatrix} 1&1&1&1&1&1&1&1&1&1&1&1&1&1&1&1 \\ 1&0&1&0&1&0&1&0&1&0&1&0&1&0&1&0 \\ 1&1&0&0&1&1&0&0&1&1&0&0&1&1&0&0 \\ 1&0&0&1&1&0&0&1&1&0&0&1&1&0&0&1 \\ 1&1&1&1&0&0&0&0&1&1&1&1&0&0&0&0 \\ 1&0&1&0&0&1&0&1&1&0&1&0&0&1&0&1 \\ 1&1&0&0&0&0&1&1&1&1&0&0&0&0&1&1 \\ 1&0&0&1&0&1&1&0&1&0&0&1&0&1&1&0 \\ 1&1&1&1&1&1&1&1&0&0&0&0&0&0&0&0 \\ 1&0&1&0&1&0&1&0&0&1&0&1&0&1&0&1 \\ 1&1&0&0&1&1&0&0&0&0&1&1&0&0&1&1 \\ 1&0&0&1&1&0&0&1&0&1&1&0&0&1&1&1 \\ 1&1&1&1&0&0&0&0&0&0&0&0&1&1&1&1 \\ 1&0&1&0&0&1&0&1&0&1&0&1&1&0&1&0 \\ 1&1&0&0&0&0&1&1&0&0&1&1&1&1&0&0 \\ 1&0&0&1&0&1&1&0&0&1&1&0&1&0&0&1 \end{bmatrix}$$

Moreover, the optical source used in our simulations is an incoherent white light source emitting a light spectrum of spectral width B equal to 12.62 nm, as shown in Fig.6. In order to encode the signal corresponding to each user and associate it with a unique code sequence, the spectrum emitted by the optical source is divided into several wavelengths, equivalent to the code length, of different values. Consequently, the spacing between adjacent wavelengths is determined by the spectrum width B divided by the length of the code (L=32) [36].

$$\Delta\lambda = \frac{B}{L} = \frac{12.68}{32} = 0.39nm \quad (20)$$

The code sequences consisting of the different wavelengths assigned to each user at the encoder and decoder are shown in the Table 3. It should be noted that

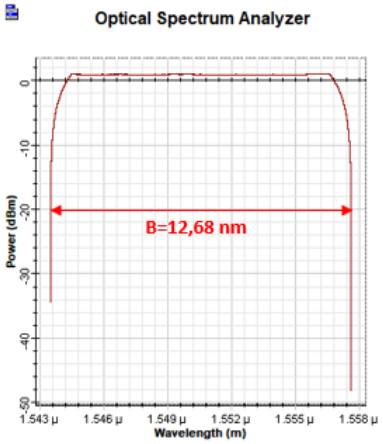

Fig. 6 Spectral band of the incoherent white light source

the code sequence corresponding to a user's encoder and decoder is the same, while that corresponding to the complementary decoder is the complementary code sequence.
Figure 7 represents the optical signal at the output of the first user's encoder. It indicates the 16 peaks corresponding to the 16 wavelengths constituting the user's specific code sequence.

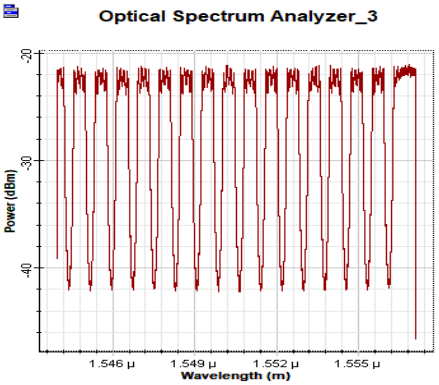

Fig. 7 Optical signal at the output of the first user's encoder

4.2.2.1 BER variation versus FBG bandwidth for different users

The first simulations regarding the investigation of the SAC-OCDMA system using the Hadamard code of length L=32, have been performed by studying the variation of the BER as a function of the bandwidth of FBGs used for signal encoding and decoding. For this purpose, we set the number of users, the data rate and the fiber distance to 11 users, 100 Mbps and 10 Km, respectively.
The results shown in Fig.8 indicate that the BER corresponding to the different users decreases for bandwidth values between 0.1 nm and 0.4 nm, and then increases

Table 3 Code sequences of each user at the encoder and the complementary decoder

	Code sequences	
	Encoder	Complementary decoder
User 1	$\lambda_1\lambda_3\lambda_5\lambda_7\lambda_9\lambda_{11}\lambda_{13}\lambda_{15}\lambda_{17}\lambda_{19}\lambda_{21}\lambda_{23}\lambda_{25}\lambda_{27}\lambda_{29}\lambda_{31}$	$\lambda_2\lambda_4\lambda_6\lambda_8\lambda_{10}\lambda_{12}\lambda_{14}\lambda_{16}\lambda_{18}\lambda_{20}\lambda_{22}\lambda_{24}\lambda_{26}\lambda_{28}\lambda_{30}\lambda_{32}$
User 2	$\lambda_1\lambda_2\lambda_5\lambda_6\lambda_9\lambda_{10}\lambda_{13}\lambda_{14}\lambda_{17}\lambda_{18}\lambda_{21}\lambda_{22}\lambda_{25}\lambda_{26}\lambda_{29}\lambda_{30}$	$\lambda_3\lambda_4\lambda_7\lambda_8\lambda_{11}\lambda_{12}\lambda_{15}\lambda_{16}\lambda_{19}\lambda_{20}\lambda_{23}\lambda_{24}\lambda_{27}\lambda_{28}\lambda_{31}\lambda_{32}$
⋮	⋮	⋮
User 32	$\lambda_1\lambda_4\lambda_6\lambda_7\lambda_{10}\lambda_{11}\lambda_{13}\lambda_{16}\lambda_{18}\lambda_{19}\lambda_{21}\lambda_{24}\lambda_{25}\lambda_{28}\lambda_{30}\lambda_{31}$	$\lambda_2\lambda_3\lambda_5\lambda_8\lambda_9\lambda_{12}\lambda_{14}\lambda_{15}\lambda_{17}\lambda_{20}\lambda_{22}\lambda_{23}\lambda_{26}\lambda_{27}\lambda_{29}\lambda_{32}$

for values from 0.4 nm to 0.6 nm. This leads us to deduce that the optimal value of the bandwidth providing a good BER performance would be 0.4 nm. The corresponding BERs for users 2, 4, 9 and 11 are 2.80E-26, 1.48E-19, 1.87E-16 and 1.86E-14, respectively.

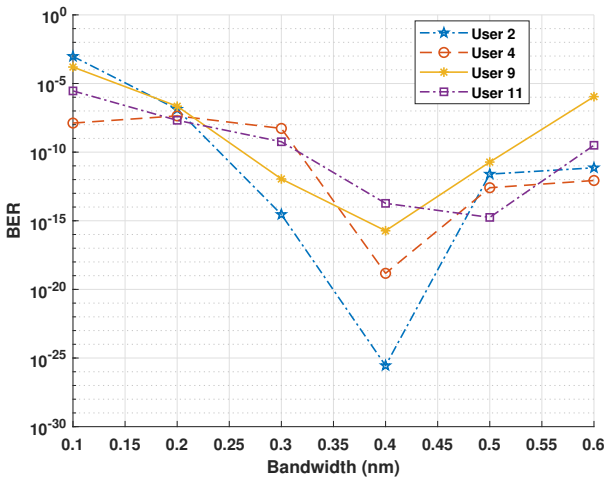

Fig. 8 BER variation versus FBG bandwidth for different users

4.2.2.2 BER, Q factor and SNR variations versus number of users for different fiber distances

This section aims to study the performance of the SAC-OCDMA system for a larger number of users. Based on the previous comparison of the obtained results in section 4.2.1 for both used codes, we have concluded that the use of the Hadamard code allows a good BER performance compared to the m-sequence code.
In this case, we are interested in studying the proposed system performance using Hadamard code of length L=32 (m=5) at a bit rate of 100 Mbits/s and a FBG bandwidth of 0.4 nm. Figure 9 and Fig.10 show respectively the BER and the Q factor as a function of the number of users for different fiber distances. It is clearly demonstrated that as the number of users and fiber distance increase, the BER increases and the Q factor decreases. Taking the first transmission distance L=5 Km, we can see that the number of possible users meeting an acceptable BER value is around 13 active users with BER=4.71E-09 and Q=6.76. Also, a good BER performance is achieved for a SAC-OCDMA system of 10 users using a fiber length of about 25 Km, the corresponding BER and Q factor values are 1.02E-09 and 7.24, respectively. At L=45 Km, the studied SAC-OCDMA system still provides good transmission performance for a total number of about 8 active users with a BER of 9.8E-09 and a Q factor of 5.82.

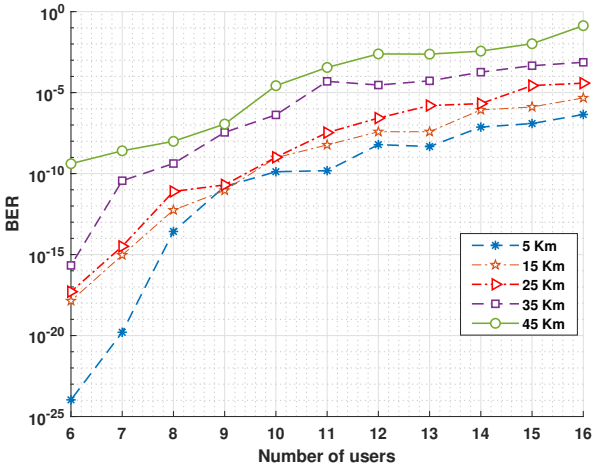

Fig. 9 BER variation versus number of users for different fiber distances for a SAC-OCDMA system using Hadamard code (L=32)

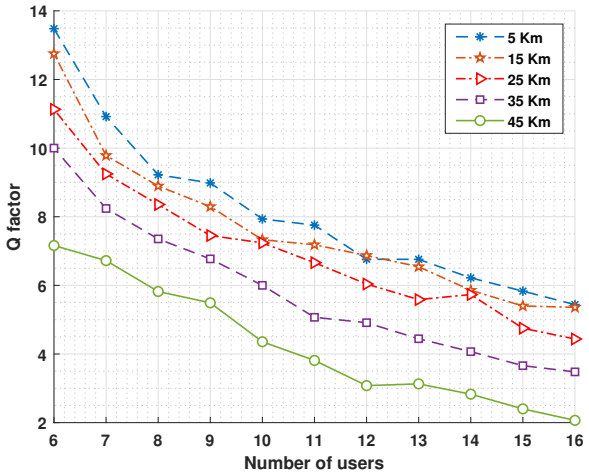

Fig. 10 Q-factor versus number of users for different fiber distances for a SAC-OCDMA system using Hadamard code (L=32)

Finally, Fig.11 shows the SNR variation against the number of active users for different fiber distances. It is obviously clear that the SNR varies non-proportionally with the number of users as well as with the fiber distance. Therefore, as the number of active users increases, the resulting noise increases and the SNR decreases. The SNR achieved at L=5 km with 6 users is about 41.11 dBm, while with 13 users it is about 27.5 dBm. Similarly, for the maximum distance of 45 km providing a good BER for up to 8 users, the SNR is also satisfactory and estimated to be around 20.71 dBm.

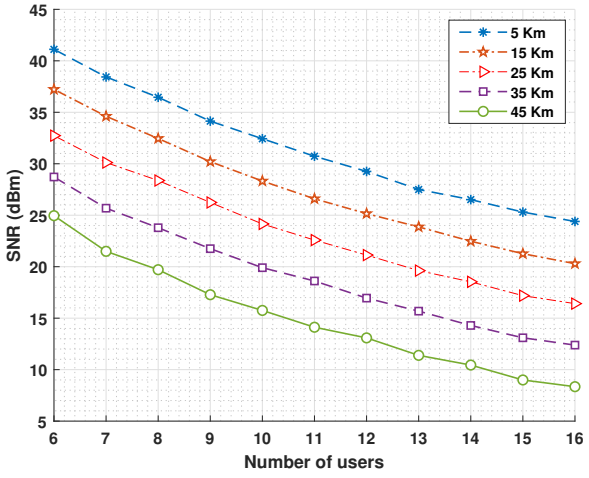

Fig. 11 SNR variation versus number of users for different fiber distances for a SAC-OCDMA system using Hadamard code (L=32)

Table 4 summarizes the different simulation results corresponding to m-sequence code and Hadamard code in terms of achieved fiber distance, number of users, BER, Q-factor and SNR.

5 Conclusion

The present paper investigates the performance of SAC-OCDMA system using two different code sequences, namely: m-sequence code and Hadamard code with use of balanced detection technique. The proposed SAC-OCDMA system performance was evaluated in terms of Q factor, BER and SNR as a function of number of active users and fiber distances. The first part of obtained results, comparing the both used code sequences for a system of 10 active users, indicates that the Hadamard code allows good BER performance and longer transmission distances compared to the m-sequence code. Then, the second part of results corresponding to the Hadamard code of length L=32, shows that the studied system remains performing for 13 active users at L= 5 Km with a bit rate of 100 Mbits/s. Also, good and acceptable Q factor, BER and SNR values are achieved for a total number of active users equals to 8 using a transmission distance of up to 45 Km. In view of these achieved performances, the proposed system can be adapted to different Multiple Access applications to meet the demands for high speeds and fast, secure services.

Acknowledgements This work is supported by CNRST Morocco under an excellence research grant.

Conflict of interest

The authors declare that they have no conflict of interest.

Data availability statement

The authors declare that all data generated or analysed during this study are included in this published article [and its supplementary information files].

References

1. I. Fsaifes, Encodage et décodage temporels" tout-optique" à réseaux de bragg pour l'accès multiple. Ph.D. thesis, Télécom ParisTech (2007)
2. S.A. Abd El Mottaleb, H.A. Fayed, A. Abd El Aziz, M.H. Aly, IOSR J Electron Commun Eng Apr **9**(2), 55 (2014)
3. K.S. Chen, Y.C. Chen, L.G. Liao, Applied Sciences **8**(12), 2408 (2018)
4. N. Kaur, R. Goyal, M. Rani, Journal of Optical Communications **38**(1), 77 (2017)

Table 4 Comparison of simulation results for m-sequence and Hadamard codes in terms of number of users, Fiber distance, BER, Q-factor and SNR

Fiber distance	m-sequence (L=15)		Hadamard (L=16)		Hadamard (L=32)			
(Km)	Number of users	BER	Number of users	BER	Number of users	BER	Q-factor	SNR (dBm)
5	9	9E-09	9	1.51E-09	13	4.71E-09	6.76	27.5
15	7	1.43E-10	8	7.28E-10	11	5.87E-09	6.81	26.6
25	7	4.33E-09	8	1.44E-09	10	1.02E-09	7.24	24.15
35	6	1.28E-09	7	1.17E-09	8	4.18E-10	7.35	23.79
45	5	1.5E-10	6	3.65E-09	8	9.79E-09	5.82	20.71
55	4	6.93E-09	5	6.38E-09				

5. A.E. Farghal, H.M. Shalaby, Journal of Optical Communications and Networking **10**(1), 35 (2018)
6. P. Prucnal, M. Santoro, T. Fan, Journal of lightwave technology **4**(5), 547 (1986)
7. A.L. Memon, K.B. Amur, A.A. Shaikh, Mehran University Research Journal of Engineering and Technology **33**(1), 103 (2014)
8. G. Kaur, S. Singh, Int. J. Eng. Sci **17**, 471 (2016)
9. R. Sahbudin, M. Abdullah, M. Mokhtar, Optical fiber technology **15**(3), 266 (2009)
10. B.C. Yeh, Optik **130**, 633 (2017)
11. K. Ghoumid, A. Ghadban, S. Boukricha, R. Yahiaoui, S. Mekaoui, M. Raschetti, C. Lepers, et al., Telecommunication Systems **73**(3), 433 (2020)
12. A. El-Mottaleb, A. Somia, H.A. Fayed, A. El-Aziz, M.A. Metawee, M.H. Aly, et al., Applied Sciences **8**(10), 1861 (2018)
13. M. Noshad, K. Jamshidi, Journal of Optical Communications and Networking **2**(6), 344 (2010)
14. J.F. Huang, C.T. Yen, Y.W. Tu, Journal of Optical Communications and Networking **2**(11), 975 (2010)
15. H. Djellab, N. Doghmane, A. Bouarfa, M. Kandouci, Journal of Optical Communications **39**(4), 381 (2018)
16. M.Z. Norazimah, S.A. Aljunid, H.M. Al-Khafaji, H.A. Fadhil, M. Anuar, in *Key Engineering Materials*, vol. 594 (Trans Tech Publ, 2014), vol. 594, pp. 1059–1065
17. M. Norazimah, S. Aljunid, H.A. Fadhil, A.M. Zain, in *2011 2nd International Conference on Photonics* (IEEE, 2011), pp. 1–5
18. K. Ghoumid, R. Ferriere, B.E. Benkelfat, B. Guizal, T. Gharbi, Journal of lightwave technology **28**(23), 3488 (2010)
19. Z. Wei, H. Ghafouri-Shiraz, H. Shalaby, IEEE Photonics Technology Letters **13**(8), 890 (2001)
20. S. Boukricha, K. Ghoumid, S. Mekaoui, E. Ar-Reyouchi, H. Bourouina, R. Yahiaoui, SN Applied Sciences **2**(6), 1 (2020)
21. S.A. Abd El-Mottaleb, H.A. Fayed, M.H. Aly, M.R. Rizk, N.E. Ismail, Optical and Quantum Electronics **51**(11), 1 (2019)
22. M. Salah, A.M. Alhassan, Evaluation **3**(1), 34 (2017)
23. M.A. Abu-Rgheff, *Introduction to CDMA wireless communications* (Academic Press, 2007)
24. S. Tseng, J. Wu, Electronics letters **44**(7), 488 (2008)
25. F. Hasoon, S. Aljunid, M. Abdullah, S. Shaari, journal of engineering science and technology **1**(2), 192 (2006)
26. S.H. Tsai, Y.P. Lin, C.C. Kuo, IEEE Transactions on Signal Processing **54**(8), 3166 (2006)
27. I.L.A. Jabbar, T.S. Mansour, International Journal of Physical Sciences **10**(16), 466 (2015)
28. K.S. Kumar, S. Sardar, A. Sangeetha, Indian Journal of Science and Technology **8**(S2), 179 (2015)
29. M. Rochette, S. Ayotte, L.A. Rusch, Journal of lightwave technology **23**(4), 1610 (2005)
30. H.M. Al-Khafaji, S. Aljunid, H.A. Fadhil, Journal of Modern Optics **59**(10), 878 (2012)
31. K. Ghoumid, I. Elhechmi, S. Mekaoui, C. Pieralli, T. Gharbi, Optics Communications **289**, 85 (2013)
32. R.S. Fyath, H.M. Ali, Journal of Emerging Trends in Computing and Information Sciences **3**(3), 444 (2012)
33. G. Keiser, *Optical communications essentials* (McGraw-Hill Education, 2003)
34. E.D. Smith, R.J. Blaikie, D.P. Taylor, IEEE Transactions on Communications **46**(9), 1176 (1998)
35. H.M. Al-Khafaji, A. SA, A. Amphawan, H.A. Fadhil, IEICE Electronics Express **10**(5), 20130044 (2013)
36. S. Ayotte, L.A. Rusch, in *LEOS 2006-19th Annual Meeting of the IEEE Lasers and Electro-Optics Society* (IEEE, 2006), pp. 911–912